JOURNAL OF AIRCRAFT
Vol. 33, No. 2, March–April 1996

Optimal Vertical Takeoff and Landing Helicopter Operation in One Engine Failure

Yiyuan Zhao* and Ali A. Jhemi†
University of Minnesota, Minneapolis, Minnesota 55455
and
Robert T. N. Chen‡
NASA Ames Research Center, Moffett Field, California 94035

This article presents optimal vertical takeoff and landing (VTOL) trajectories of a multiengine helicopter in the event of a single engine failure. A point-mass model of the UH-60A helicopter is used. Time derivatives of thrust coefficients are treated as control variables. A first-order response dynamics is assumed for the contingency power available after an engine failure. Ground effect is included in the study of landing trajectories. A linear backup procedure is assumed for normal takeoff and a straight-in procedure for normal landing. Nonlinear optimal control problems are formulated for flights of rejected takeoff, continued takeoff, continued landing, and balked landing after one engine failure. Constraints on rotor speed and thrust vector are included. In rejected takeoff and continued landing, the cost functional minimizes the distance between the touchdown point and the original takeoff point, subject to impact speed limits at touchdown. In continued takeoff and balked landing, two cost functionals are used subject to specified final speed components required for a steady climb. One minimizes the horizontal distance required to achieve the steady climb, whereas the other maximizes the minimum altitude during the transitional flight from engine failure to the steady climb. Extensive numerical solutions are obtained. In all optimal trajectories, the helicopter adjusts its power requirement to accommodate the contingency power available. The helicopter gross weight capability in VTOL operation is limited by safe rejected takeoff or continued landing. A concept of balanced-weight takeoff and landing decision point is proposed from which the maximum gross weight in emergency landing and in flying-out maneuver is the same.

Nomenclature

C_P = power coefficient
C_T = thrust coefficient
C_z, C_x = thrust coefficient components
c_d = mean profile drag coefficient of rotor blades
f_e = equivalent flat plate area for fuselage
f_G = ground effect factor
H_R = rotor hub height when the helicopter is on ground
h, x = vertical, horizontal position, ft
I_R = rotor polar moment of inertia, slug ft^2
K_{ind} = induced power factor
P_{OEI} = maximum one engine inoperative power available, shaft hp
P_s = available shaft power, shaft hp
P_{TO} = one engine maximum normal takeoff power
R = main rotor radius, ft
T = main rotor thrust, lb
$\bar{U}_c$, $\bar{U}_t$ = normalized flow components at the main rotor
U_2 = horizontal component of V_{TOSS} or V_{BLSS}, ft/s
u_z, u_x = modified control variables
V = airspeed, ft/s
V_{BLSS} = balked landing safety speed, ft/s
V_{TOSS} = takeoff safety speed, ft/s
v = induced velocity in ground effect, ft/s
$\bar{v}_i$ = normalized uniform rotor induced velocity
W = helicopter gross weight, mg, lb
w, u = vertical, horizontal velocity component, ft/s
β = thrust vector inclination, deg
γ = takeoff slope/approach angle, deg
η = power efficiency factor
θ_w = angle between rotor wake and a vertical reference line
λ = inflow ratio
ρ = air density, slug/ft^3
σ = rotor solidity ratio
τ_p = turboshaft engine time constant, s
Ω = rotor angular speed, rad/s

Subscripts
max = maximum value allowed
min = minimum value allowed
0 = initial values at engine failure

Received June 9, 1995; presented as Paper 95-3178 at the AIAA Guidance, Navigation, and Control Conference, Baltimore, MD, Aug. 7–10, 1995; revision received Sept. 26, 1995; accepted for publication Sept. 27, 1995.

*Assistant Professor, Department of Aerospace Engineering and Mechanics. Member AIAA.
†Ph.D. Candidate, Center for Control Sciences.
‡Civil Rotorcraft Group Leader, Rotorcraft and Powered Lift Branch.

I. Introduction

HELICOPTERS are known for their vertical takeoff and landing (VTOL) capability. VTOL flight modes are necessary for operations from oil rigs, city-center buildings, and other confined heliports. This article studies optimal VTOL helicopter flight trajectories in the event of a single engine failure and examines the associated heliport size requirement and maximum gross weight capability.

Depending on its flight characteristics in engine failure, a transport helicopter with a gross weight of 6000 lb or more can be certified as either category A or category B.[1] The category B certification applies to either single engine or multiengine helicopters with a gross weight of less than 20,000 lb, and requires that a safe landing be possible in the case of one or all engine failures. On the other hand, the category A certification applies to multiengine helicopters with indepen-

dent engine systems and requires that a helicopter be able to either continue flight or land safely in the event of a single engine failure. Strictly speaking, only category A helicopters are allowed to operate from confined areas and/or to fly en route over areas with no emergency landing sites.

The Federal Aviation Administration (FAA) regulations require a category A helicopter to take specific actions in the event of one engine failure[1] (Fig. 1). If one engine becomes inoperative (OEI) during a takeoff before the helicopter reaches the takeoff decision point (TDP), the pilot must reject the takeoff (RTO) to land safely. If OEI occurs after the TDP, the pilot must continue the takeoff (CTO). In a landing flight, the pilot must continue the landing (CL) if an engine fails after the helicopter has passed the landing decision point (LDP). The pilot may either continue or balk the landing (BL) if the engine failure occurs before the LDP. If no engine fails, the helicopter should proceed with normal takeoff or landing. In VTOL operations, confined heliports require that a helicopter land back close to the original takeoff point.

In the past, Lande[2] discussed various takeoff and landing procedures used by helicopter pilots on oil rigs over the North Sea. These include static takeoff, dynamic takeoff, straight-in landing, and sideway ascent/descent. Vodegel and Stevens[3] developed a computer program for the certification of category A helicopter VTOL operation. Goldenberg et al.[4] proposed the systematic use of the sideway ascent/descent procedure for the M230 helicopter on an elevated helipad. Wood et al.[5] further discussed various details of the sideway ascent/descent procedure.

Applying nonlinear optimal control theory, Okuno and Kawachi[6] studied vertical takeoff flight trajectories of a helicopter in the case of one engine failure. For rejected takeoff flight, problems were formulated to minimize the impact speed at touchdown and to maximize helicopter gross weight for engine failure occurring at the worst possible height. For continued takeoff flight the problem was formulated to maximize the minimum altitude.

Research efforts were also made to understand category A runway helicopter operation. Saal and Cole[7] used comprehensive flight tests to study category A takeoff and landing procedures of the S-76B helicopter. Cerbe and Reichert[8] studied optimal category A takeoff flight for the BO 105 helicopter using a static power required field model. Okuno and Kawachi[6] studied choices of TDP velocity and takeoff slope for runway length reduction using nonlinear optimal control theory. Zhao and Chen[9] determined category A takeoff trajectories of a UH-60A helicopter to minimize runway lengths and to maximize gross weight. Sharma et al.[10,11] studied runway landing of the UH-60A helicopter. Furthermore, Studwell[12] developed a general computer program for evaluating helicopter performances. Partial or total power loss at any point along a flight path can be simulated. Jepson[13] proposed a method to compute takeoff and landing characteristics of a twin-engine helicopter following an engine failure. In addition, autorotative landings after a complete power failure[14-16] have been studied.

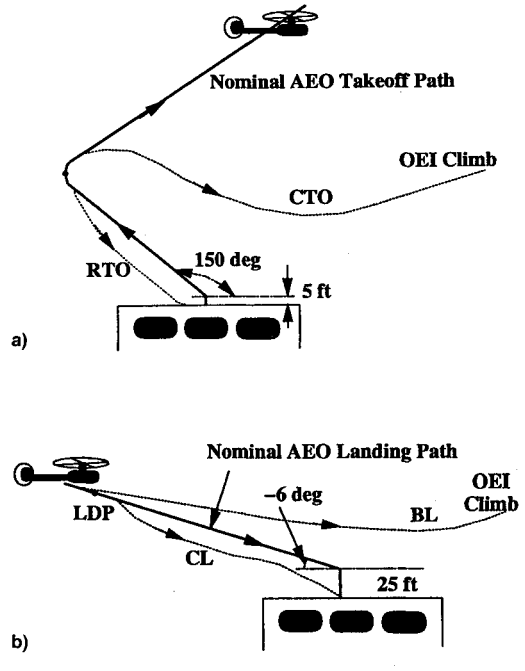

Fig. 1 Nominal AEO flight in VTOL operation: a) takeoff and b) landing.

Despite these advances, more studies are needed to reveal the basic characteristics, heliport configuration requirement, and gross weight capability in a VTOL operation in the event of one engine failure. This article presents optimal category A VTOL flight paths that minimize heliport size, subject to path constraints and terminal conditions derived from helicopter structure/aerodynamic limitations and the FAA safety standards.

In the rest of this article, a summary of the equations of motion and various constraints for a two-dimensional point mass helicopter model are given. FAA rules and piloting procedures for category A VTOL operation are then discussed. Results on rejected takeoff and continued takeoff are presented next in detail, followed by results on continued landing. These results are compared in Sec. VII and are summarized in Sec. VIII.

II. Helicopter Modeling

A two-dimensional point-mass model for the UH-60A helicopter is employed.[9,14,15] The equations of motion are repeated here for convenience:

$$m\dot{w} = mg - \rho(\pi R^2)(\Omega R)^2 C_z - \tfrac{1}{2}\rho f_e w\sqrt{u^2 + w^2} \tag{1}$$

$$m\dot{u} = \rho(\pi R^2)(\Omega R)^2 C_x - \tfrac{1}{2}\rho f_e u\sqrt{u^2 + w^2} \tag{2}$$

$$I_R\Omega\dot{\Omega} = P_s - (1/\eta)\rho(\pi R^2)(\Omega R)^3 C_P \tag{3}$$

$$\dot{h} = -w \tag{4}$$

$$\dot{x} = u \tag{5}$$

where the thrust coefficients are defined as

$$T = \rho(\pi R^2)(\Omega R)^2 C_T \tag{6}$$

$$C_z = C_T \cos\beta \tag{7}$$

$$C_x = C_T \sin\beta \tag{8}$$

The airspeed and flight-path angle are

$$V = \sqrt{u^2 + w^2} \tag{9}$$

$$\sin\gamma = -(w/V) \tag{10}$$

Time derivatives of C_z and C_x are employed as control variables. A first-order response dynamics of the contingency power available is assumed for turboshaft engines:

$$\dot{C}_z = u_z \tag{11}$$

$$\dot{C}_x = u_x \tag{12}$$

$$\dot{P}_s = (1/\tau_p)(P_{\text{OEI}} - P_s) \tag{13}$$

In this point-mass model there are eight states: w, u, Ω, h, x, C_z, C_x, and P_s; two controls: u_z and u_x; and two control parameters: P_{OEI} and m.

Initial state conditions for flights in an engine failure mode are determined from the all engine operating (AEO) takeoff or landing path immediately prior to the engine failure. In particular, the initial values of thrust coefficients and power are solved from Eqs. (1–3) assuming a nominal AEO path. AEO flight paths must be specified so that the initial power value is less than the maximum AEO power limit.

The required power coefficient is computed from

$$C_P = C_T\sqrt{(C_T/2)}(K_{\text{ind}} f_G \bar{v}_i + \bar{U}_c) + \tfrac{1}{8}\sigma c_d \tag{14}$$

where

$$\bar{U}_c = \frac{u \sin\beta - w\cos\beta}{\Omega R\sqrt{C_T/2}} \tag{15}$$

$$\bar{U}_t = \frac{u\cos\beta + w\sin\beta}{\Omega R\sqrt{C_T/2}} \tag{16}$$

and the ideal normalized induced velocity is given by the

$$\bar{v}_i = \begin{cases} 1/\sqrt{\bar{U}_t^2 + (\bar{U}_c + \bar{v}_i)^2} & (2\bar{U}_c + 3)^2 + \bar{U}_t^2 > 1 \\ \bar{U}_c(0.373\bar{U}_c^2 + 0.598\bar{U}_t^2 - 1.991) & \text{otherwise} \end{cases} \tag{17}$$

In these relations, $\bar{v}_i$, $\bar{U}_c$, and $\bar{U}_t$ are normalized by the mean rotor-induced velocity at hover.

In the previous set of equations, rotor speed dynamics in Eq. (3) are based on Talbot et al.[17] and Johnson.[18] The first relation in Eq. (17) is the momentum theory for rotor-induced velocity. The second relation, given by Johnson,[14] is an empirical approximation to the induced velocity in the vortex-ring state. The required power coefficient in Eq. (14) and momentum theory are discussed in Schimtz,[19] Gessow and Myers,[20] and Stepniewski and Keys.[21]

In Eq. (14), $f_G \leq 1$ accounts for the ground effect. In general, benefits of ground effect are most pronounced at hover and decrease gradually as the horizontal speed increases. Cheeseman and Bennett[22] proposed a simple source model to account for induced velocity decrease in ground effect in forward flight.

However, flight test evidence indicates a power surge as the helicopter just starts to develop level speed (Ref. 23). To explain this phenomenon, Curtiss et al.[24] used a moving rotor experiment and identified two distinct flow regions around the rotor at low forward speeds: 1) a recirculation and 2) a ground vortex region. The recirculation region causes the induced velocity at the leading edge of the rotor to increase, resulting in induced power increase. The ground vortex region suppresses the full development of induced velocity. As the helicopter's forward speed increases, the recirculation region diminishes. Based on these results, Cerbe et al.[25] proposed a modification to the Cheeseman and Bennett[22] source model that includes the effect of the recirculation region. Decker et al.[26] showed that the time constant for the induced velocity dynamics is on the order of $\tau \approx 0.21/|\lambda|\Omega_0$. This time constant is much smaller compared to the flight time associated with the critical phases of takeoff and landing. Therefore, induced velocity response time is ignored.

In this article, ground effect is included for rejected takeoff and continued landing. For simplicity, the source model by Cheeseman and Bennett[22] is used. We have[14]

$$f_G = 1 - \frac{R^2\cos^2\theta_w}{16(h + H_R)^2} \tag{18}$$

where

$$\cos^2\theta_w = \frac{(-wC_T + vC_z)^2}{(-wC_T + vC_z)^2 + (uC_T + vC_x)^2} \tag{19}$$

$$v = K_{\text{ind}} v_h \bar{v}_i f_G \tag{20}$$

The aerodynamic and structural limitations of rotor blades result in constraints on the rotor speed, the rotor thrust, and the thrust angle:

$$\Omega_{\min} \leq \Omega \leq \Omega_{\max} \tag{21}$$

$$C_{T_{\min}} \leq C_T \leq C_{T_{\max}} \tag{22}$$

$$\beta_{\min} \leq \beta \leq \beta_{\max} \tag{23}$$

Traditionally, the OEI contingency power ratings include a 2.5- and a 30-min power rating. Since the first 30 s are the most critical phase after an engine failure, a 30-s supercontingency power followed by a 2-min contingency power is proposed[27] and used.[28] In the current study, we assume that the maximum OEI power for the first 30 s is 115% of the AEO takeoff power: $P_{\text{OEI}} = 1.15P_{\text{TO}}$. We also assume that the power from the failing engine drops to zero instantaneously. In reality, this power decays over a short period of time.

The Sikorsky UH-60A (Black Hawk) helicopter[29–31] is used as the example helicopter. This single rotor helicopter is powered by two T700-GE-700 turboshaft engines. The Appendix lists some important parameters of this helicopter as well as parameters used in the optimization studies.

For numerical solutions of the nonlinear optimal control problems formulated next, the sequential gradient restoration algorithm developed by Miele et al.[32] is used. This algorithm can treat path and terminal constraints only in equality form. Therefore, slack variables[33] are used to convert path inequality constraints in Eqs. (21–23) into equalities. Slack parameters are also used to convert terminal inequality constraints, discussed next, into equalities. A Newton–Raphson scheme is used to solve the ideal normalized induced velocity in the first relation of Eq. (17), with an initial guess of 1.0 and a stepsize of 0.8. The ground effect induced velocity is also obtained with a Newton–Raphson scheme, where the initial guess is the ideal induced velocity and the stepsize is one. In the numerical solution process, all distances are normalized by $(10R)$ and time by $100/\Omega_0$.

III. VTOL Helicopter Operation

Specific takeoff and landing procedures in VTOL operation depend on the heliport type. In an oil rig platform, a helicopter can descend below the heliport deck to fly out or land on the water in an emergency. Therefore, it can takeoff vertically and the TDP height is usually low (20 ft, Lande[2]). In a static takeoff the helicopter climbs with a small airspeed and zero acceleration. In a dynamic pulling-up it climbs with a vertical acceleration. In a city-center or a confined ground level heliport the helicopter must fly back to the original takeoff spot in an emergency, and the nominal AEO takeoff path should allow the pilot to see the heliport at all times. As a result, a linear backup is usually employed. In an elevated heliport the helicopter can descend below the heliport deck in continued takeoff or balked landing. For a ground level heliport, the helicopter must stay well above the ground during flying out. Normal landing paths are similar in all cases and involve a straight-in flight with a constant flight-path angle and a constant speed reduction. At a certain height above the heliport the helicopter descends vertically to the heliport surface.

In addition to VTOL operations performed in a two-dimensional vertical plane, lateral takeoff and landings are also used by pilots over the North Sea[2] and studied for systematic op-

eration of the M230 helicopter.[4,5] In this procedure, a helicopter on takeoff would ascend laterally to the decision point above and to the side of the heliport. During a normal landing, the helicopter would first fly to this sideway point and then descend laterally to the heliport. If an engine fails when the helicopter is between the decision point and the heliport, the pilot should land. If OEI occurs beyond the decision point, the pilot should fly out.

In any case, FAA requires that the helicopter be able to land safely if OEI occurs at any point up to TDP on takeoff or at any point during landing. The helicopter must be able to continue flight if the OEI occurs after TDP on takeoff or before LDP on landing.

This article focuses on VTOL operation from either a city-center or a ground-level confined heliport. In other words, the helicopter must return to the heliport for an emergency landing. Figure 1 shows nominal AEO takeoff and landing flight paths used in this article. These nominal AEO paths are selected based on recommended procedures for the UH-60A and the Super Puma helicopter.

In the nominal AEO takeoff path, the helicopter starts by hovering in ground effect. Then, the pilot would increase the collective and adjust power to follow a steady linear backup climb ($\gamma_0 = 150$ deg, $V_0 = 5$ kn, $\dot{V} = 0$) to the takeoff decision point. At any point before TDP, the horizontal location is given by

$$x_0 = -\sqrt{3}(h_0 - 5) \tag{24}$$

Around the TDP, the helicopter flies vertically up briefly before climbing out.

In the nominal AEO landing, the helicopter approaches the heliport with a constant glide-path angle of (−6 deg) and a constant deceleration of ($-0.0755\ g$). It has a speed of 35 kn at $h = 100$ ft and reaches zero speed at $h = 25$ ft. At 25 ft above the heliport surface, the helicopter starts to descend vertically. The horizontal location is determined from

$$x_0 = -[(h_0 - 25)/\tan 6\ \text{deg}] \tag{25}$$

The deceleration at any point along the nominal path is given by

$$\dot{V}_0 = -0.0755\ g = -2.4311\ \text{ft/s}^2 \tag{26}$$

IV. Rejected Takeoff Flight

During a successful RTO, the helicopter must return to the heliport and land with reasonable speeds. Therefore, we formulate an optimal control problem to minimize the dispersions of touchdown points, subject to specified touchdown speed limits. The origin of the coordinate system lies in the original takeoff point:

$$\min_{u_z, u_x} I = x^2(t_f) \tag{27}$$

subject to

$$h(t_f) = 0 \tag{28}$$

$$u(t_f) \leq U_{\max} \tag{29}$$

$$w(t_f) \leq W_{\max} \tag{30}$$

where t_f is open and $W_{\max} = 5$ ft/s.[29] With a ($-0.2\ g$) deceleration, the helicopter stopping distance is given by

$$d = U_{\max}^2/0.4\ g \tag{31}$$

In this study, $U_{\max} = 15$ ft/s. Preliminary calculations show that Eq. (30) can be either active or inactive, depending on helicopter gross weights and initial conditions. For consistency, Eq. (30) is enforced as an equality.

Figure 2 shows the optimal RTO trajectories for engine failure occurring at different heights for $W = 16{,}000$ lb, $P_{\text{OEI}} = 1656$ hp, $V_0 = 5$ kn $= 8.4$ ft/s, and $\gamma_0 = 150$ deg. At these conditions, the helicopter can always return close to the original takeoff point in rejected takeoffs. The touchdown point deviates the most from the origin for initial height around 40–60 ft. This is consistent with a typical H–V diagram. The airspeed decreases as the helicopter turns around and then gradually increases. For engine failures at low altitudes, the vertical descent rate and airspeed reach the maximum limit at touchdown point. For engine failures occurring at high altitudes, the helicopter has time to develop a larger descent rate before touchdown and the airspeed reaches a peak during the flight.

The helicopter reduces its power requirement to accommodate the OEI power available. As a result, the rotor angular speed reduces to the lower limit upon engine failure. A helicopter requires less power at a higher speed up to the best rate of climb speed. For higher engine failure altitudes, the helicopter can build up airspeed to reduce the power requirement. The rotor speed increases after the initial reduction to store energy in the rotor. This energy is used toward the end to cushion the landing. For lower engine failure altitudes, the helicopter does not have enough altitude range to develop sufficient airspeed for reducing the power requirement. The rotor speed has to stay at the lower limit to reduce profile power. The thrust coefficient increases gradually until at the end, where it decreases and the rotor speed increases due to the ground effect.

Time histories of the rotor angular speed reveal the gross weight capability of the helicopter for a given OEI power level. Figure 3 shows the effect of helicopter gross weight on the optimal RTO trajectories for $P_{\text{OEI}} = 1656$ hp, $V_0 = 5$ kn, $\gamma_0 = 150$ deg, and with $W = 15{,}000$, 15,700, 16,000, and 16,300 lb. For a larger gross weight, the rotor speed stays at the lower limit for a longer portion of the flight and the final rotor speed is lower. As the gross weight increases, both airspeed and descent rate reach higher peaks during the flight. No feasible solutions can be obtained if the gross weight is increased further. Therefore, the maximum gross weight is defined by a rotor speed history that stays at the lower limit to the end.

Investigations are also made by using higher OEI power levels and by formulating the problem to minimize touchdown speeds with a constraint on touchdown point location. Results indicate that a larger limit of vertical descent rate or horizontal velocity component at touchdown allows a helicopter to carry more payload. However, the most effective way of increasing gross weight capability is by increasing the OEI contingency power available after an engine failure.

Ground effect plays an important role in low-speed landing, especially for helicopters with large rotors such as the UH-60A. We also calculated optimal RTO paths at the same conditions as in Fig. 2 without ground effect. A feasible solution cannot be obtained with $W = 16{,}000$ lb when there is no ground effect. A much lower weight has to be used. Therefore, one should consider the presence of ground effect in estimating the maximum payload a helicopter can carry. For VTOL operation from a ground-level confined heliport, ground effect is usually present. On building-top heliports, however, the ground effect is not always as pronounced. For consistency, all optimal trajectories of rejected takeoff and continued landing in this article are computed with ground effect included.

V. Continued Takeoff and Balked Landing Flight

A continued takeoff must be possible for engine failures occurring at any point after TDP. FAA regulations specify that at the end of a continued takeoff transition flight, the helicopter

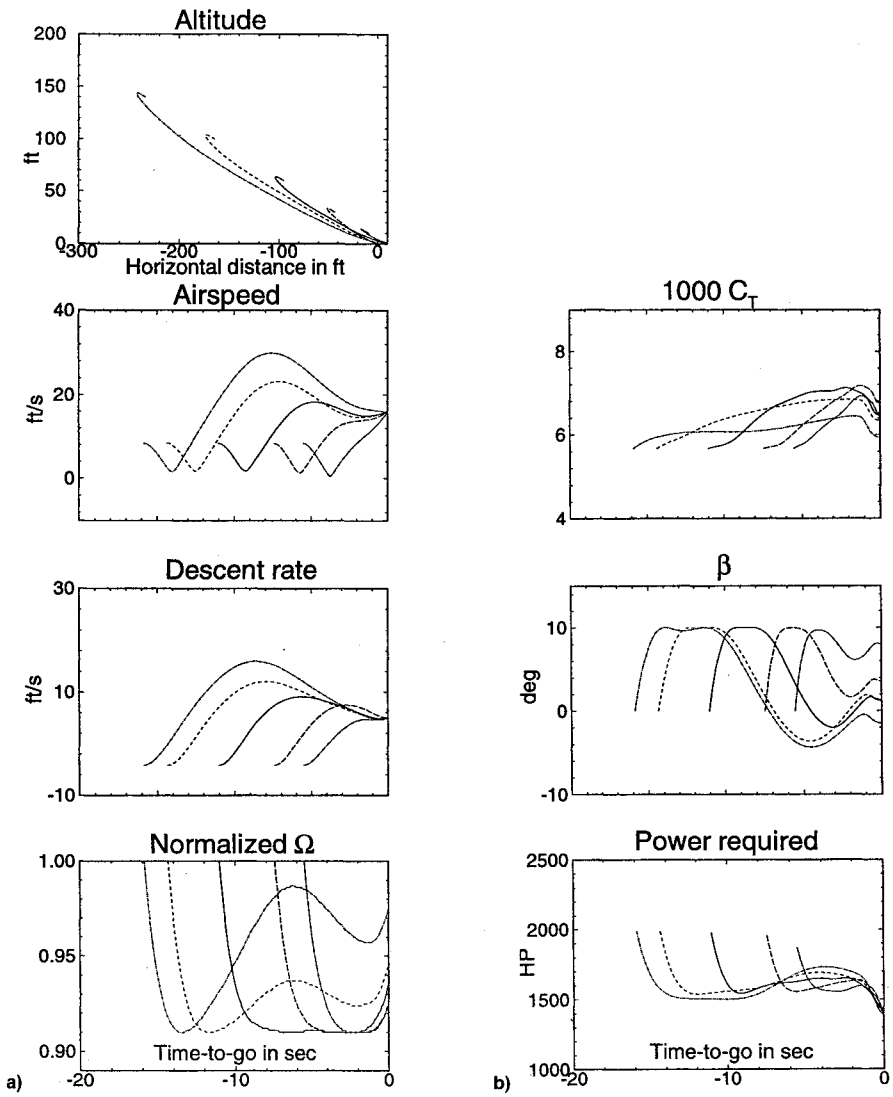

Fig. 2 Optimal RTO trajectories with W = 16,000 lb, P_{OEI} = 1656 hp, V_0 = 8.4 ft/s, and γ_0 = 150 deg: a) states and b) thrust and required power.

achieve 1) a minimum of 35 ft above the takeoff surface (or above the sea level in operation from an oil rig), 2) a minimum of 100 fpm climb rate, and 3) a preselected takeoff safety speed V_{TOSS}.

In a continued takeoff, there is a tradeoff among helicopter gross weight capability, heliport adjacent space requirement, and minimum altitude during the transition flight after engine failure to the steady OEI climb. For a given gross weight, the helicopter can fly to minimize the required horizontal space or to increase the minimum altitude. We have

$$\min_{u_z,u_x} I = x(t_f) \tag{32}$$

or

$$\max_{u_z,u_x} \min_{t} h(t) \tag{33}$$

subject to

$$h(t_f) \geq 35 \text{ ft} \tag{34}$$

$$-w(t_f) \geq 100 \text{ fpm} \tag{35}$$

$$u(t_f) \geq U_2(W) \text{ ft/s} \tag{36}$$

$$\dot{w}(t_f) = 0 \tag{37}$$

$$\dot{u}(t_f) = 0 \tag{38}$$

$$\dot{\Omega}(t_f) = 0 \tag{39}$$

The last three conditions are included to guarantee a steady-state flight at the end of the continued takeoff transition.

If thrust coefficients were used as controls, these terminal constraints would directly contain control variables. As a result, derivatives of the thrust coefficients are employed as control variables to formulate the trajectory optimization problems into a standard nonlinear optimal control framework. The use of these modified control variables also forces the thrust coefficients to be continuous at the initial time, partially simulating pilot response delays.

As pointed out by Johnson,[34] the cost functional in Eq. (33) can be approximated by

$$\min I = \int_{t_0}^{t_f} (H_{ref} - h)^q \, dt \tag{40}$$

where q is an even integer and H_{ref} is a reference height well above the altitude history. In this article, $H_{ref} = h_0 + 100$ ft, and q = 6 and then 8.

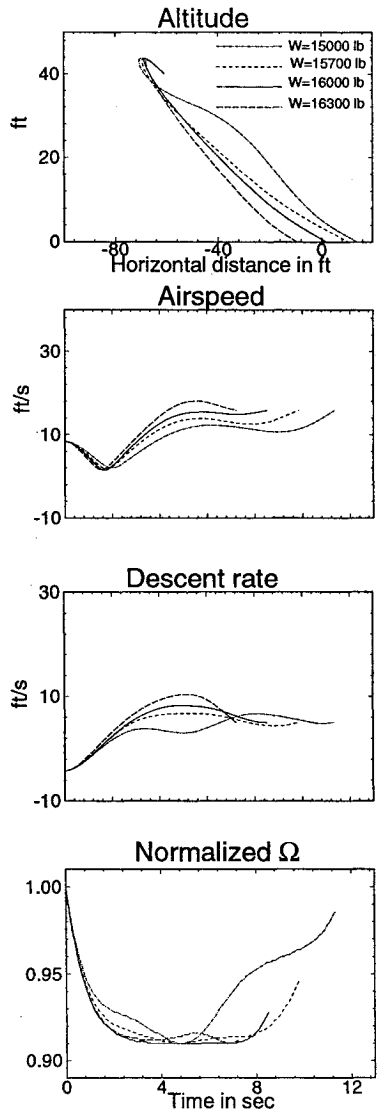

Fig. 3 Effect of helicopter gross weight in RTO, P_{OEI} = 1656 hp, V_0 = 8.4 ft/s, and γ_0 = 150 deg.

In Eq. (36) U_2 is the horizontal component of V_{TOSS} and is usually much larger than 100 fpm:

$$V_{TOSS} = \sqrt{U_2^2 + w^2(t_f)} \approx U_2 \tag{41}$$

Helicopters require less power at larger forward speeds below a certain limit. As a result, U_2 must be high enough for the helicopter to carry a certain weight in a steady OEI climb at a certain power level. Therefore, Eq. (36) is included as a terminal constraint to provide consistency between the continued takeoff transition after an engine failure and the steady OEI climb. The relation between U_2 and W is determined from the steady-state solutions of Eqs. (1–3). In this article, we assume that P_{OEI} = 1656 hp and rotor speed in steady OEI climb is the nominal rotor speed. Any lower rotor speed within limits allows for a larger gross weight.

Figure 4 shows the optimal CTO trajectories at three initial altitudes for minimizing the final distance and for maximizing the minimum altitude. The flight conditions correspond to W = 16,572 lb, V_0 = 2 ft/s, γ_0 = 90 deg, and U_2 = 45.75 ft/s. In maximizing the minimum altitude, the helicopter trades all possible rotor rotational energy to gain airspeed and altitude. As a result, the rotor speed reduces to and stays at the minimum limit. The airspeed increases monotonically to reach the specified value. As the initial altitude changes, the optimal altitude histories simply shift vertically, while all other states stay the same.

In contrast, optimal CTO trajectories for minimizing the final distance are different for different initial altitudes. As the initial altitude increases, peak descent rate increases and the rotor angular speed reaches higher values in the middle of the flight. Both total flight time and horizontal distance become shorter. To minimize the final distance, the helicopter descends to trade potential energy for airspeed and for rotor rotational energy. Toward the end, the helicopter pulls up by using the rotational energy reserve to meet the climb conditions. For all three initial altitudes, the final altitude is the same and equal to 35 ft.

Actually, as the initial altitude becomes higher than a certain limit, optimal CTO trajectories for minimizing $x(t_f)$ also become the same: the altitude histories simply shift vertically while other state histories remain the same. In other words, there is a maximum altitude drop that the helicopter needs to gain sufficient airspeed.

On the other hand, there is a minimum required altitude drop at each gross weight that the helicopter needs simply to satisfy constraints and reach the terminal conditions. With this altitude drop the two performance indices produce identical results. For W = 16,572 lb, optimal CTO trajectories for minimizing $x(t_f)$ and those for maximizing the minimum altitude become the same at h_0 = 100 ft. Therefore, the minimum altitude drop for W = 16,572 lb at V_0 = 2 ft/s is about Δh = 100 − 35 = 65 ft. Higher initial airspeeds require a smaller altitude drop for the same weight.

Figure 5 demonstrates the tradeoff among gross weight, horizontal space, and minimum altitude. The conditions are P_{OEI} = 1656 hp, V_0 = 2 ft/s, γ_0 = 90 deg, h_0 = 100 ft, and U_2 = 38.75, 42.25, 45.75 ft/s, respectively for W = 15,856, 16,209, and 16,572 lb. At a smaller weight, the helicopter can minimize the horizontal distance required to achieve the steady OEI climb at the expense of a low minimum altitude, or to raise the altitude history by using a larger horizontal space. As the gross weight increases, the requirement for achieving the desired OEI climb conditions dominates the solution and the two types of optimal trajectories become the same. Any higher gross weight at these conditions would cause the helicopter to violate some of the constraints. Further increase in gross weight capability is possible through higher OEI power level, higher initial altitude, therefore altitude drop range, or a larger initial airspeed.

If γ_0 = 150 deg is used in the initial conditions instead, optimal CTO trajectories start with a backward swing motion. Nonetheless, all of the previous conclusions are valid. Actually, different initial flight-path angles do not affect the continued takeoff paths significantly at low speeds. Because pilots would like to fly forward immediately in continued takeoff after an engine failure, a brief vertical climb segment is included around TDP in the nominal AEO takeoff path shown in Fig. 1a. Therefore, γ_0 = 90 deg is used in this article. Since the airspeed and altitude increase in a nominal AEO takeoff path after TDP, continued takeoff becomes easier if the engine failure occurs at a later time in the normal takeoff.

The previous trajectories can also be used to construct CTO flight paths for engine failures at low altitudes. One can simply connect a steady OEI climb segment to the end of the trajectories to reach a 35-ft clearance. The required horizontal distance needs to be increased accordingly.

A balked landing must be possible for engine failures at any point prior to the landing decision point along the nominal AEO landing path. The same conditions are required at the end of a balked landing transition flight as in a continued takeoff, except for the use of V_{BLSS}. Actually, V_{BLSS} and V_{TOSS} are often selected to be the same.

The results of balked landing flights after an engine failure are found to be generally similar to a continued takeoff. However, balked landing has some unique features. Because of high

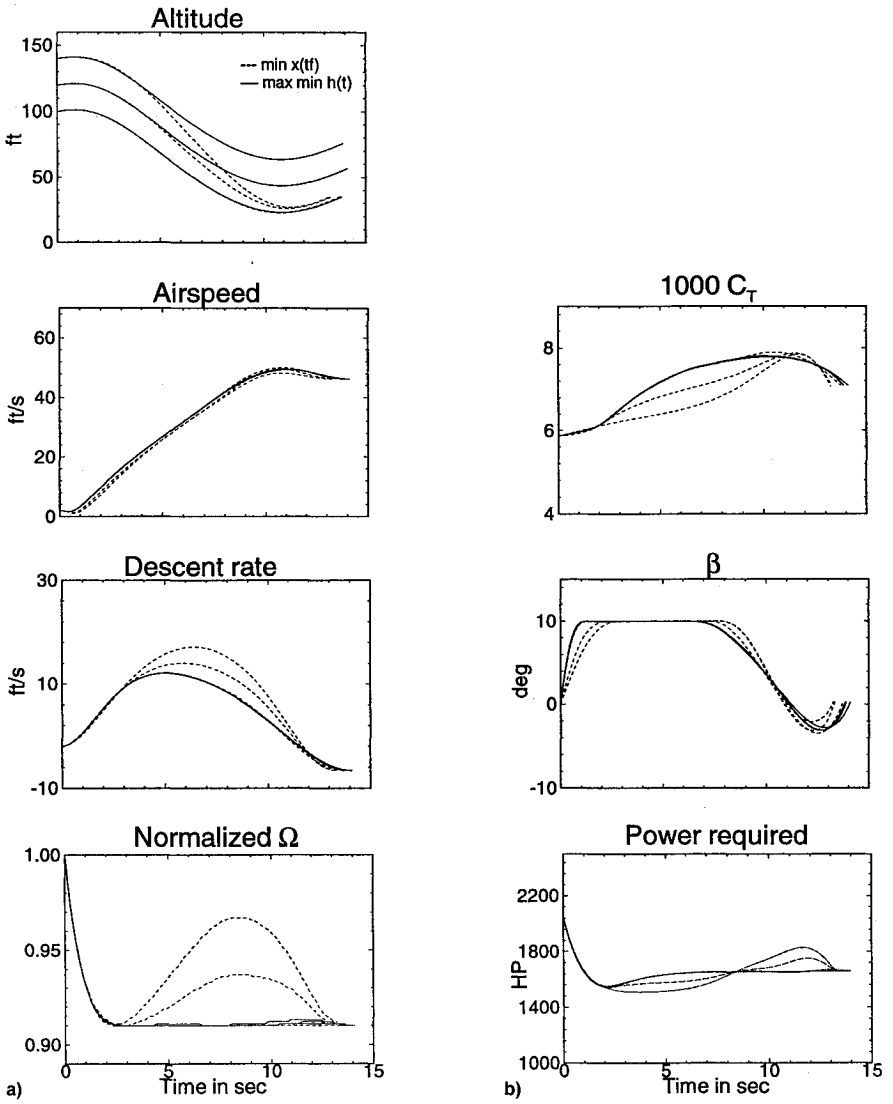

Fig. 4 Optimal CTO paths with W = 16,572 lb, P_{OEI} = 1656 hp, V_0 = 2.0 ft/s, γ_0 = 90 deg, and U_2 = 45.75 ft/s: a) states and b) thrust and required power.

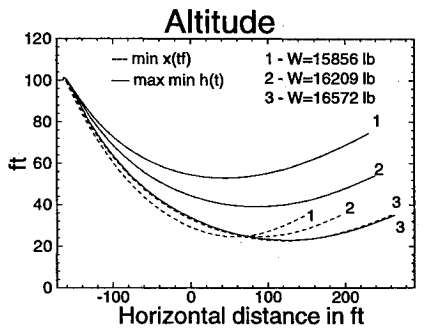

Fig. 5 Effect of gross weights in CTO with P_{OEI} = 1656 hp, V_0 = 2.0 ft/s, and γ_0 = 90 deg.

initial airspeeds, a balked landing for engine failure occurring at higher altitude allows for a much larger gross weight compared to continued landing. These results are similar to those found for the short takeoff and landing operation.[11] Since the airspeed decreases along the nominal AEO landing path, the maximum gross weight possible in a balked landing reduces significantly as the altitude decreases.

VI. Continued Landing Flight

For continued landing in OEI, we again calculate trajectories to minimize the heliport size requirement as in Eq. (27), subject to Eqs. (28–30). If the final descent speed becomes negative in the optimization, optimal trajectories are recalculated where Eq. (30) is enforced as an equality with $w(t_f) = 0$. This prevents the helicopter from descending below the takeoff reference level during the flight.

Figure 6 shows a continued landing in OEI with W = 16,000 lb, P_{OEI} = 1656 hp, and $\gamma_0 = -6$ deg. The optimal continued landing trajectories are very different for engine failures occurring at different altitudes. At h_0 = 100 ft and V_0 = 35 kn = 56 ft/s, the OEI power level is larger than the power required in the nominal AEO landing. This is because the power available from the remaining engine is automatically increased to the maximum OEI level after an engine failure. As a result, the helicopter faces power excess in OEI and has to increase its power requirement to match the OEI power available. Correspondingly, the rotor speed increases during the flight. A similar situation occurs for h_0 = 80 ft and V_0 = 50.6 ft/s. As the initial altitude and airspeed decrease along the nominal AEO landing path, the nominal power required increases and continued landing flights in OEI are gradually characterized by power deficiency. For (h_0 = 60 ft and V_0 = 40.4 ft/s), and lower altitudes and airspeed, the rotor speed in a continued landing reduces to and stays at the lower limit until the end, where it increases due to the ground effect. Along the nominal AEO landing path, airspeed becomes zero at h_0 = 25 ft. Continued landing after an engine failure at h_0 = 25 ft is a pure vertical descent, consistent with the autorotation flight dis-

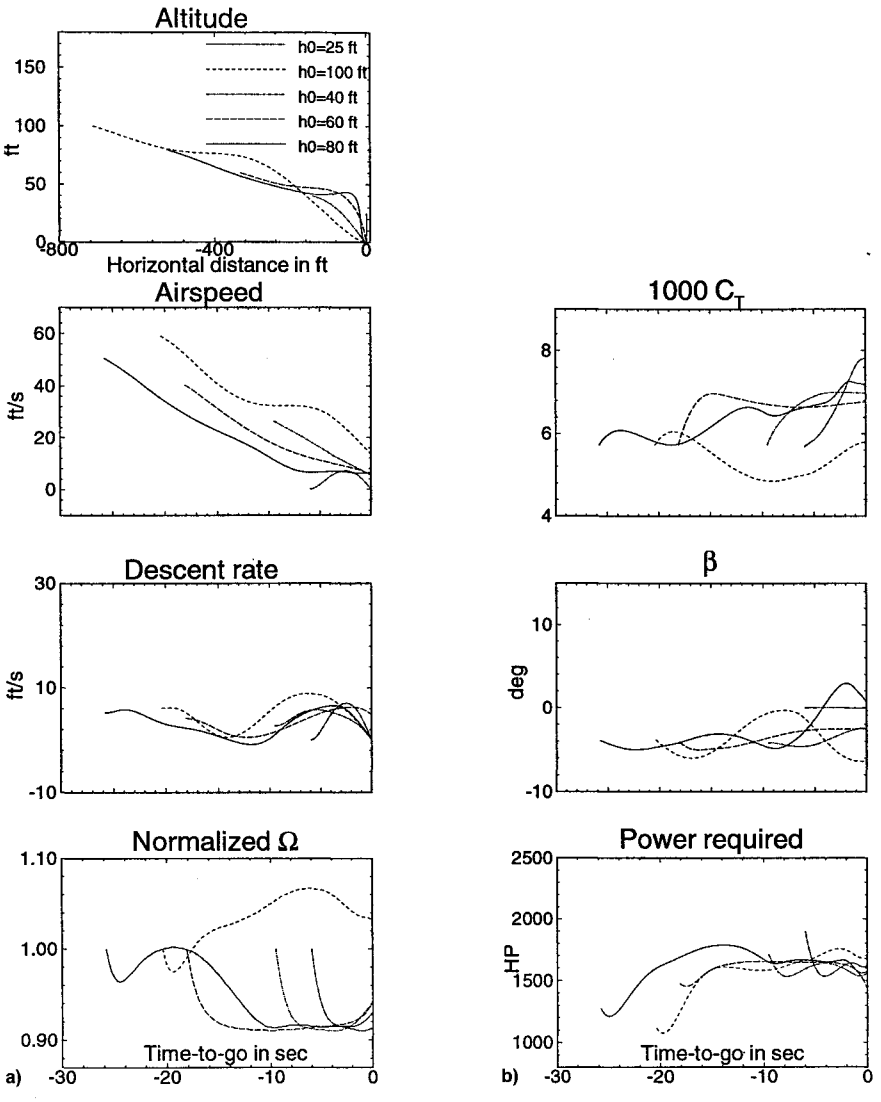

Fig. 6 Optimal CL paths with W = 16,000 lb, P_{OEI} = 1656 hp, and $\gamma_0 = -6$ deg: a) states and b) thrust and required power.

cussed in Refs. 14 and 15. Continued landing flights from lower altitudes are also vertical and become easier as initial altitude decreases.

Along the nominal AEO landing path considered, the maximum gross weight possible is limited by continued landing at lower initial altitudes. In particular, no feasible solutions can be obtained with a gross weight of 16,500 lb or higher for continued landing starting at h_0 = 25 ft and V_0 = 0. On the other hand, much larger gross weight is possible for continued landing starting at higher initial altitudes and airspeeds. This bottle-neck phenomenon is a manifestation of the H–V diagram of a helicopter. Again, higher OEI power levels and/or larger limits for the vertical descent rate at touchdown allow for larger gross weights.

VII. Discussion

Optimal OEI trajectories are shaped by proper energy management and flight constraints. In the usual cases of deficiency in available OEI power, the helicopter reduces its power requirement to accommodate the power available in an engine failure. In the case of excess in available OEI power, the helicopter increases its power requirement to match the power available. For example, in rejected takeoff and in continued landing at low initial altitudes, the helicopter power requirement decreases to a level close to the OEI power available after an engine failure. Reduction in power requirement is accomplished by increased airspeed and decreased rotor angular speed. In continued landing at high altitudes and speeds the helicopter increases its power requirement to use all of the OEI power available; as a result, the rotor angular speed increases after the initial reduction.

For the specified nominal AEO VTOL operation paths and a given OEI power, the gross weight capability of a helicopter is determined by the rejected takeoff and continued landing flight phases. The maximum gross weight possible in rejected takeoff or continued landing is limited by the high power requirement at low speeds and by the typical shape of an H–V diagram. Airspeeds become necessarily low in these cases because the helicopter needs to land on the helipad. The gross weight capability for both cases can be increased by using a higher OEI power level. On the other hand, one can increase the maximum gross weight possible in either continued takeoff or balked landing simply by increasing the decision point height.

One can select locations of the TDP to achieve balanced gross weight capability for RTO and CTO. Rejected takeoffs are most difficult for engine failures at a certain band of altitudes reflective of the H–V diagram. Above this altitude range it becomes easier to land a helicopter in OEI. Since it must be possible to make a safe rejected takeoff at any point up to the takeoff decision point, there is no advantage or disadvantage to locate TDP very high once it passes the critical altitude band. Psychologically, it may be difficult for the pilot to make a safe landing from a high altitude. In comparison, the maxi-

mum gross weight in a continued takeoff increases as the TDP height increases. Since the gross weight capability in a VTOL operation is determined by the lower gross weight in RTO or CTO, we recommend the use of a balanced-weight height for TDP. At this height, the maximum gross weight in CTO is about the same as that in RTO. In other words, the takeoff decision point only needs to be high enough to allow the helicopter to fly out safely at the maximum gross weight possible for rejected takeoff. A similar concept holds for the landing decision point.

In this article, it is assumed that the contingency power of the remaining engine increases exponentially to the maximum OEI power level after the other engine fails. In most cases such as rejected takeoff, continued takeoff, and balked landing, helicopter flight after an engine failure is a power deficiency problem. In continued landing from high initial altitudes and airspeed, on the other hand, the helicopter power required is actually less than the maximum OEI power available. In the latter case, one could vary the OEI power available to provide just enough power required by the helicopter to follow the nominal AEO landing path. Since the power required varies along the nominal AEO path, varying OEI power in an engine failure emergency could add complexity to the pilot operation. Besides, safe landing can be achieved with excess powers if the rotor speed is allowed to vary. For simplicity, therefore, it is reasonable to assume that the OEI power increases to the maximum possible upon an engine failure. This practice simplifies pilot action. In fact, FAA requires that the pilot only use primary flight controls in the first 2.5 min after an engine failure. Use of balanced-weight decision points can reduce the number of power excess cases.

No specific values of TDP or LDP height are discussed, because proper choices of these heights should be based on an accurate helicopter model. While the point-mass model is useful in studying basic tradeoffs in a category A helicopter operation, more sophisticated models are required to refine the results obtained earlier.

It is clear that the nominal AEO flight path in takeoff or landing plays a crucial role in shaping optimal OEI trajectories. As a result, AEO flight paths affect the maximum gross weight capability and heliport requirements in OEI flights. Further studies are needed to determine all-engine-operating flight paths that are optimal for OEI flights. A rigid-body helicopter model needs to be used.

VIII. Conclusions

This article presents optimal helicopter flight trajectories in the event of one engine failure in a VTOL operation. Flights of rejected takeoff, continued takeoff, continued landing, and balked landing after an engine failure are formulated as nonlinear optimal control problems. A point-mass model of the UH-60A helicopter is used and realistic constraints on rotor speed and thrust vector are included. A first-order response dynamics is used for the contingency power available after an engine failure. Ground effect is included in the study of landing trajectories. A linear backup procedure is assumed for normal takeoff and a straight-in procedure for normal landing. In rejected takeoff and continued landing, deviations of the touchdown point from the original takeoff spot are minimized, subject to safe touchdown speed limits. In continued takeoff and balked landing, two cost functionals are considered subject to terminal conditions corresponding to a steady OEI climb. One minimizes the horizontal distance and the other maximizes the minimum altitude.

Extensive numerical solutions are obtained at various conditions of engine failure and helicopter gross weight. In computed optimal flight trajectories, the helicopter maneuvers to match its power requirement to the level of the OEI contingency power available. In the usual cases of deficient OEI power available, optimal trajectories reduce the power requirement to accommodate the OEI power loss. In continued landing at high initial altitudes and speeds, the helicopter increases its power requirement to use all of the excess OEI power available.

In a rejected takeoff or a continued landing, the maximum gross weight possible is limited by engine failures occurring at a certain range of altitudes close to the helipad. This is reflective of a typical H–V diagram. In a continued takeoff or balked landing with a given gross weight, one has the choice of maximizing the minimum altitude or minimizing the horizontal distance. As the gross weight increases, the two types of optimal trajectories produce identical results. Further increase in gross weight capability can be achieved through higher altitude range of maneuver, higher initial airspeed, or higher OEI power. As a result, the gross weight capability in category-A VTOL operation for a given OEI power level is fundamentally limited by rejected takeoff and continued landing flight phases after an engine failure. Higher OEI power levels can increase the gross weight capability.

Height of the takeoff decision point can be selected so that the maximum gross weight possible in continued takeoff and in rejected takeoff is about the same. This balanced-weight height concept also applies to the landing decision point.

Appendix: UH-60A Parameters for Optimization Studies

The UH-60A helicopter has a maximum takeoff weight of 22,000 lb. The maximum takeoff power is 3086 SHP. Other related parameters are $R = 26.83$ ft, $\sigma = 0.0821$, $\Omega_0 = 27$ rad/s, $C_{T_{max}} = 0.1846$, $I_R = 7060$ slug ft^2, and $H_R = 12.33$ ft.

Values of parameters used in the optimizations are $f_e = 30$ ft^2, $\rho = 0.002377$ slug/ft^3, $g = 32.2$ ft/s^2, $c_d = 0.012$, $\eta = 0.90$, $K_{ind} = 1.15$, $\beta_{max} = 10$ deg, $\beta_{min} = -10$ deg, $\bar{\Omega}_{max} = 107\%$, $\bar{\Omega}_{min} = 91\%$, $\tau_p = 1.5$ s, and $P_{TO} = 1440$ hp. The thrust constraints used in the optimizations are $C_{T_{min}} = 0.002$ and $C_{T_{max}} = 0.025$; these limits are not encountered in the optimization process.

Acknowledgments

The work is supported through a cooperative agreement between NASA Ames Research Center and the University of Minnesota under NCC2-809. We thank the Supercomputer Institute at the University of Minnesota for granting its supercomputer resources.

References

[1]"Certification of Transport Category Rotorcraft," Federal Aviation Administration, Advisory Circular AC-29A, 1987.

[2]Lande, K., "New Offshore Helicopter Rig Takeoff and Landing Procedures," *Proceedings of 1989 Experimental Test Pilot Symposium*, 1989, pp. 179–204.

[3]Vodegel, H. J. G. C., and Stevens, J. M. G. F., "A Computer Program for the Certification of Helicopter Vertical Takeoff and Landing Operations and an Application to the S-76B Helicopter," *47th Annual Forum of the American Helicopter Society* (Phoenix, AZ), American Helicoper Society, Washington, DC, 1991, pp. 721–731.

[4]Goldenberg, J., Meslin, L., Blondino, M., and Williams, D., "Certification of Model 230 Helicopter for Category 'A' Elevated Helipad Operations," *Proceedings of the American Helicopter Society 49th Annual Forum* (St. Louis, MO), American Helicopter Society, Washington, DC, 1993, pp. 1497–1505.

[5]Wood, T. L., Blondino, M., and Williams, D., "M230 Helicopter Performance for Category A Elevated Helipad Operation," *19th European Rotorcraft Forum* (Cernobbio, Italy), 1993, pp. 01-1–01-11 (Paper 01).

[6]Okuno, Y., and Kawachi, K., "Optimal Takeoff of a Helicopter for Category A STOL/VTOL Operations," *Journal of Aircraft*, Vol. 30, No. 2, 1993, pp. 235–240.

[7]Saal, K. W., and Cole, J. L., "Category 'A' Certification of S-76B Featuring Variable CDP and V2 Speeds," *Journal of the American Helicopter Society*, Vol. 35, No. 3, 1990, pp. 12–21.

[8]Cerbe, T., and Reichert, G., "Optimization of Helicopter Takeoff and Landing," *Journal of Aircraft*, Vol. 26, No. 10, 1989, pp. 925–

931.

[9]Zhao, Y., and Chen, R. T. N., "Critical Considerations for Helicopters During Runway Takeoffs," *Journal of Aircraft*, Vol. 32, No. 4, 1995, pp. 773–781.

[10]Sharma, V., "Optimal Helicopter Operation from a Clear Heliport in the Event of One Engine Failure," Ph.D. Dissertation, Dept. of Aerospace Engineering and Mechanics, Univ. of Minnesota, MN, Nov. 1994.

[11]Sharma, V., Zhao, Y., Chen, R. T. N., and Hindson, W. S., "Optimal OEI Clear Heliport Operation of a Multiengine Helicopter," *Proceedings of the American Helicopter Society 51st Forum* (Dallas, TX), American Helicopter Society, Washington, DC, 1995.

[12]Studwell, R. E., "Helicopter Dynamic Performance Program, Volume I. Engineer's Manual," USARTL-TR-79-27A, National Technical Information Service AD-A088 474/2, July 1980.

[13]Jepson, W. D., "Some Considerations of the Landing and Takeoff Characteristics of Twin-Engine Helicopters, Part II—Heliport Size Requirements," *Journal of the American Helicopter Society*, Vol. 8, April 1963, pp. 35–50.

[14]Johnson, W., "Helicopter Optimal Descent and Landing After Power Loss," NASA TM 73244, May 1977.

[15]Lee, A. Y., Bryson, A. E., and Hindson, W. S., "Optimal Landing of a Helicopter in Autorotation," *Journal of Guidance, Control, and Dynamics*, Vol. 11, No. 1, 1988, pp. 7–12.

[16]Okuno, Y., Kawachi, K., Azuma, A., and Saito, A., "Analytical Prediction of Height-Velocity Diagram of a Helicopter Using Optimal Control Theory," *Journal of Guidance, Control, and Dynamics*, Vol. 14, No. 2, 1991, pp. 453–459.

[17]Talbot, P. D., Tinling, B. E., Decker, W. A., and Chen, R. T. N., "A Mathematical Model of a Single Main Rotor Helicopter for Piloted Simulation," NASA TM-84281, Sept. 1982.

[18]Johnson, W., *Helicopter Theory*, Princeton Univ. Press, Princeton, NJ, 1980, pp. 282, 283.

[19]Schimtz, F., "Aerodynamics of Helicopters," Stanford Univ., AA 230 Class Notes, Stanford, CA, 1991.

[20]Gessow, A., and Myers, G. C., Jr., *Aerodynamics of the Helicopter*, Frederick Ungar Publishing Co., New York, 1952.

[21]Stepniewski, W. Z., and Keys, C. N., *Rotary-Wing Aerodynamics*, Dover, New York, 1984.

[22]Cheeseman, I. C., and Bennett, N. E., "The Effect of the Ground on a Helicopter Rotor in Forward Flight," NASA Ames Research Center Rept. 3021, 1955.

[23]Prouty, R. W., *Helicopter Performance, Stability, and Control*, Krieger, Malabar, FL, 1990.

[24]Curtiss, H. C., Jr., Sun, M., Putman, W. F., and Hanker, E. J., "Rotor Aerodynamics in Ground Effect at Low Advance Ratios," *Journal of the American Helicopter Society*, Vol. 29, No. 1, 1984.

[25]Cerbe, T., Reichert, G., and Curtiss, H. C., Jr., "Influence of Ground Effect on Helicopter Takeoff and Landing Performance," *14th European Rotorcraft Forum* (Milano, Italy), 1988, pp. 70-1–70-17 (Paper 70).

[26]Decker, W. A., et al., "Model Development and the Use of Simulator for Investigating Autorotation," FAA Conf. on Helicopter Simulation, Atlanta, GA, April 1984.

[27]Hirschkron, E., Martin, E., and Samanich, N., "Powerplant Design for One Engine Inoperative Operation," *Vertiflite*, Vol. 30, No. 5, 1984, pp. 34–38.

[28]Trivier, D., and Bosqui, O., "30-Second/2-Minute One Engine Inoperative Certification for the AS 332 Super Puma MK II," *18th European Rotocraft Forum* (Avignon, France), 1992, pp. 129-1–129-15.

[29]"Operator's Manual: UH-60A and EH-60A Helicopters," Dept. of the Army, TM 55-1520-237-10, Jan. 1988.

[30]Howlett, J. J., "UH-60A Black Hawk Engineering Simulation Program," Vol. I, NASA CR-166309, Dec. 1981.

[31]Hilbert, K. B., "A Mathematical Model of the UH-60 Helicopter," NASA TM 85890, April 1984.

[32]Miele, A., Damoulakis, J. N., Cloutier, J. R., and Tietze, J. L., "Sequential Gradient Restoration Algorithm for Optimal Control Problems with Non-Differential Constraints," *Journal of Optimization Theory and Applications*, Vol. 13, No. 2, 1974, pp. 218–255.

[33]Jacobson, D. H., and Lele, M. M., "A Transformation Technique for Optimal Control Problems with a State Variable Inequality Constraint," *IEEE Transactions on Automatic Control*, Vol. AC-14, No. 5, Oct. 1969, pp. 457–464.

[34]Johnson, C. D., "Optimal Control with Chebyshev Minimax Performance Index," *Journal of Basic Engineering*, Vol. 89, Series D, No. 2, 1967, pp. 251–262.